JCTC Journal of Chemical Theory and Computation

Article

pubs.acs.org/JCTC

Physical Meaning of Virtual Kohn–Sham Orbitals and Orbital Energies: An Ideal Basis for the Description of Molecular Excitations

R. van Meer, O. V. Gritsenko, and E. J. Baerends*

Faculty of Exact Sciences, Theoretical Chemistry, VU University, 1081 HV Amsterdam, The Netherlands

Supporting Information

ABSTRACT: In recent years, several benchmark studies on the performance of large sets of functionals in time-dependent density functional theory (TDDFT) calculations of excitation energies have been performed. The tested functionals do not approximate exact Kohn–Sham orbitals and orbital energies closely. We highlight the advantages of (close to) exact Kohn–Sham orbitals and orbital energies for a simple description, very often as just a single orbital-to-orbital transition, of molecular excitations. Benchmark calculations are performed for the statistical average of orbital potentials (SAOP) functional for the potential [*J. Chem. Phys.* **2000**, *112*, 1344; **2001**, *114*, 652], which approximates the true Kohn–Sham potential much better than LDA, GGA, mGGA, and hybrid potentials do. An accurate Kohn–Sham potential does not only perform satisfactorily for calculated vertical excitation energies of both valence and Rydberg transitions but also exhibits appealing properties of the KS orbitals including occupied orbital energies close to ionization energies, virtual-occupied orbital energy gaps very close to excitation energies, realistic shapes of virtual orbitals, leading to straightforward interpretation of most excitations as single orbital transitions. We stress that such advantages are completely lost in time-dependent Hartree–Fock and partly in hybrid approaches. Many excitations and excitation energies calculated with local density, generalized gradient, and hybrid functionals are spurious. There is, with an accurate KS, or even the LDA or GGA potentials, nothing problematic about the "band gap" in molecules: the HOMO–LUMO gap is close to the first excitation energy (the optical gap).

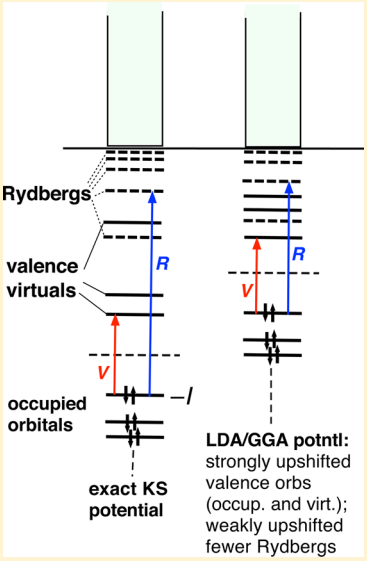

I. INTRODUCTION

Extensive sets of density functional theory (DFT) functionals have recently been tested for excitation energy calculations with adiabatic time-dependent DFT (TDDFT), for both valence and Rydberg excitations.[1−13] There is a tendency to favor hybrid functionals such as PBE0 and M06-2X as the ones with the smallest mean absolute error and the most even-handed treatment of both valence and Rydberg excitations. It has been concluded that most functionals with a large percentage (>40%) of exact exchange can describe both types of excitations correctly. In this letter, it is shown that even though these functionals generate fairly accurate excitation energies, the simple single orbital excitation structure (transition of one occupied orbital to one virtual orbital), which is characteristic for the exact Kohn–Sham orbitals[14] and which is of great importance for the correct interpretation of the nature of the excited states, is not maintained. It is shown in section II that the exact Kohn–Sham potential, as approximated with the SAOP potential (statistical average of orbital potentials functional for the potential),[15−17] generates, with a simple adiabatic local-density approximation (ALDA) exchange-correlation kernel, excitation energies that are comparable to the best functionals that were found in the benchmark studies. More importantly, as we will demonstrate in section III, the SAOP orbitals, being good approximations to the exact Kohn–Sham orbitals, also in the unoccupied spectrum, have the important advantage of describing many excitations as simple single orbital transitions. This is very helpful in understanding the nature of the excitations in a molecule. In contrast, the use of exact exchange leads to much less suitable unoccupied orbitals: they are too diffuse, and one typically needs a linear combination of many of these virtual orbitals to describe the receiving orbital in the excitation. This is, of course, the case for the Hartree–Fock model, but this less fortunate feature of that model persists to some extent in the hybrid functionals of DFT.

II. BENCHMARKING THE SAOP POTENTIAL FOR VERTICAL EXCITATION ENERGIES

In adiabatic TDDFT, the excitation energies are obtained as eigenvalues of the diagonalization of the TDDFT response equations

$$(\varepsilon^2 + 2\sqrt{\varepsilon}\mathrm{K}\sqrt{\varepsilon})\mathbf{F} = \omega^2\mathbf{F} \quad (1)$$

The ε matrix contains KS orbital energy differences on the diagonal entries

$$\varepsilon_{ia,jb} = (\epsilon_a - \epsilon_i)\delta_{ij}\delta_{ab} \quad (2)$$

Received: August 10, 2014

   dx.doi.org/10.1021/ct500727c | *J. Chem. Theory Comput.* XXXX, XXX, XXX–XXX

and the coupling matrix **K** is given by[18]

$$K_{ia,jb} = 2\int \mathrm{d}r_1 \mathrm{d}r_2 \varphi_i(r_1)\varphi_a(r_1)\left[\frac{1}{|r_{12}|} + f_{\mathrm{xc}}^{\mathrm{ad}}(r_1, r_2)\right]\varphi_j(r_2)\varphi_b(r_2) \tag{3}$$

The orbitals $\{\phi_i\}$ are KS orbitals and $f_{\mathrm{xc}}^{\mathrm{ad}}$ is the adiabatic exchange-correlation kernel, which is defined as the functional derivative of the exchange-correlation potential (v_{xc}) with respect to the density (ρ), $f_{\mathrm{xc}}^{\mathrm{ad}}(r_1, r_2) = \delta v_{\mathrm{xc}}(r_1)/\delta\rho(r_2)$. The KS orbital energies are obtained from the usual Kohn−Sham equations

$$(\hat{h}(\mathbf{r}_1) + v_{\mathrm{H}}(\mathbf{r}_1) + v_{\mathrm{xc}}(\mathbf{r}_1))\varphi_i(\mathbf{r}_1) = \epsilon_i\varphi_i(\mathbf{r}_1) \tag{4}$$

where $\hat{h}(r_1)$ is the one electron operator, $v_{\mathrm{H}}(r_1)$ is the Hartree potential and $v_{\mathrm{xc}}(r_1)$ is the exchange-correlation potential which is generated by taking the functional derivative of the exchange-correlation energy functional with respect to the density, $\delta E_{\mathrm{xc}}/\delta\rho(r_1)$. It should be noted that one only needs v_{xc} and its derivative $f_{\mathrm{xc}}^{\mathrm{ad}}$ to generate excitation energies (and other response properties such as (hyper)polarizabilities), knowledge of $E_{\mathrm{xc}}[\rho]$ is not required to generate these quantities, nor is it required for the self-consistent optimization of the KS orbitals. However, the potential v_{xc} are usually derived from existing ground state functionals for E_{xc} by functional differentiation. Most, if not all, of the currently known approximate ground state energy functionals yield an incorrect v_{xc} potential. It is well-known that the approximate LDA and GGA functionals generate deficient v_{xc} behavior in both the bulk (core and valence) region and the asymptotic region. It is customary to refer to the wrong asymptotic behavior of the GGA Kohn−Sham potentials as the main cause of problems with molecular properties.[19−24] This may be true for some properties, such as polarizabilities and hyperpolarizabilities,[20,25] and van der Waals interactions,[26,27] but perhaps a more important deficiency of the approximate KS potentials is the fact that in the bulk region the $v_{\mathrm{xc}}^{\mathrm{GGA}}$ are shifted upward by an almost constant value of ca. 4.5 eV with respect to the exact KS potential.[19,28,29] We will return to these problems with the GGA potentials below, but we first verify that the SAOP potential, which lacks these deficiencies, gives an accurate representation of the excitation energies. To that end, we have performed TDDFT calculations on the same benchmark set that was used in the calculations by Caricato et al.[6] and by Isegawa et al.[9]

The approximate SAOP xc potential $v_{\mathrm{xc}\sigma}^{\mathrm{SAOP}}$[15−17] is designed to model the KS potential both in the inner region (including the characteristic step structure in the exact KS potential[30]) and in the outer region with its Coulombic asymptotics. To this end, $v_{\mathrm{xc}\sigma}^{\mathrm{SAOP}}$ is constructed with a seamless interpolation between the model xc potential of van Leeuwen and Baerends (LB)[19] $v_{\mathrm{xc}\sigma}^{\mathrm{LB}\alpha}$ with the Coulombic asymptotics in the outer region and the model xc potential of Gritsenko, van Leeuwen, van Lenthe, and Baerends (GLLB)[30]

$$v_{\mathrm{xc}\sigma}^{\mathrm{GLLB}}(\mathbf{r}) = \bar{v}_{\mathrm{xc}\sigma}^{\mathrm{hole}}(\mathbf{r}) + \sum_{i=1}^{N_\sigma}\sqrt{\epsilon_{N\sigma} - \epsilon_{i\sigma}}\frac{|\varphi_{i\sigma}(\mathbf{r})|^2}{\rho_\sigma(\mathbf{r})} \tag{5}$$

in the bulk. The step structure is modeled in eq 5 with its second term, while the first term is a model coupling-constant integrated xc-hole potential. A seamless interpolation between $v_{\mathrm{xc}\sigma}^{\mathrm{GLLB}}$ and $v_{\mathrm{xc}\sigma}^{\mathrm{LB}\alpha}$ in $v_{\mathrm{xc}\sigma}^{\mathrm{SOAP}}$ is carried out in a 2-fold way. First, for each occupied orbital ϕ_i the auxiliary model potential $v_{\mathrm{xci}\sigma}^{\mathrm{mod}}$ is constructed with exponential interpolation between $v_{\mathrm{xc}\sigma}^{\mathrm{GLLB}}$ and $v_{\mathrm{xc}\sigma}^{\mathrm{LB}\alpha}$

$$v_{\mathrm{xci}\sigma}^{\mathrm{mod}}(\mathbf{r}) = \mathrm{e}^{-2(\epsilon_{N\sigma}-\epsilon_{i\sigma})}v_{\mathrm{xc}\sigma}^{\mathrm{LB}\alpha}(\mathbf{r}) + \{1 - \mathrm{e}^{-2(\epsilon_{N\sigma}-\epsilon_{i\sigma})}\}v_{\mathrm{xc}\sigma}^{\mathrm{GLLB}}(\mathbf{r}) \tag{6}$$

Finally, the SAOP xc potential is constructed as the statistical average of the potentials (eq 6) for the occupied orbitals

$$v_{\mathrm{xc}\sigma}^{\mathrm{SAOP}}(\mathbf{r}) = \sum_{i=1}^{N_\sigma} v_{\mathrm{xci}\sigma}^{\mathrm{mod}}(\mathbf{r})\frac{|\varphi_{i\sigma}(\mathbf{r})|^2}{\rho_\sigma(\mathbf{r})} \tag{7}$$

The SAOP functional, to the best of our knowledge, is only available in the ADF package. The ADF package uses Slater type orbitals, while the previously mentioned benchmark calculations use Gaussian basis sets. We have therefore selected a basis set (QZ3P-2D) that resembles the Gaussian basis sets in terms of the number of diffuse *s* (H) and *s*, *p* (C,N,O) functions and is larger in the *s*,*p* and polarization functions, and contains extra *d*,*f* diffuse functions. For simplicity we always use the adiabatic LDA kernel for the LDA and GGA calculations, which are not sensitive to this choice of kernel.[23] In view of the analytical form of the SAOP potential, which is reminiscent of, for example, the KLI approximation of the exchange-only OEP potential, a derivation along the lines of the derivation in refs 31 and 32 for the OEP kernel might provide an approximation to the kernel, but in view of the minor effect of the kernel (see also below), the usefulness of such an approximation to $f_{\mathrm{xc}}^{\mathrm{SAOP}}$ would seem doubtful. For the calculations with hybrid functionals the kernels are given by

$$f_{\mathrm{xc}}^{\mathrm{HYB}} = (1 - X)f_{\mathrm{xc}}^{\mathrm{ALDA}} + Xf_{\mathrm{xc}}^{\mathrm{HF}} \tag{8}$$

where X is the fraction of exact exchange used in the exchange-correlation functional.

A summary of the benchmark results is given in Table 1, while the actual excitation energies can be found in the Supporting Information. The partitioning in valence (V) and Rydberg (R) excitation is taken from the benchmark papers.[6,9] The M06-2X and BP86 calculations that have been published with 6-311(2+,2+)G** and 6-311(3+,3+)G** basis sets respectively, which we will abbreviate as Gaussian-2D and Gaussian-3D, have been repeated with the Slater QZ3P-2D basis set. The Slater basis gives, with the BP86 and M06-2X functionals, similar average absolute deviations (AADs) as the Gaussian bases, demonstrating the rough equivalence of these basis sets. This allows us to compare the SAOP results using the Slater QZ3P-2D basis with the benchmark results of other

Table 1. Average Absolute Errors for the Benchmark Calculations[a]

func.	basis	total	V	R	alkenes + carbonyls	aza-benzenes
BP86	Gaussian-3D	1.08	0.38	1.62	1.44	0.41
BP86	QZ3P-2D	1.04	0.36	1.56	1.38	0.51
M06-2X	Gaussian-2D	0.30	0.36	0.26	0.26	0.39
M06-2X	QZ3P-2D	0.32	0.34	0.31	0.33	0.31
SAOP	QZ3P-2D	0.34	0.25	0.41	0.38	0.27

[a]The BP86 calculations with Gaussian-3D (6-311(3+,3+)G**) basis sets refer to the benchmark studies by Caricato et al.[6] and M06-2X Gaussian-2D (6-311(2+,2+)G**) calculations are from Isegawa et al.[9] The benchmark set of molecules is the same as in refs 6 and 9. All errors are in electron volts.

dx.doi.org/10.1021/ct500727c | J. Chem. Theory Comput. XXXX, XXX, XXX−XXX

functionals in the previously mentioned studies. The total AAD of the SAOP functional is 0.34 eV, which indicates that SAOP is a reasonably successful functional, comparable to M06-2X with AAD 0.32 in the same basis. SAOP is a functional with good AAD for both the valence and the Rydberg excitations. This also holds true for the M06-2X hybrid functional, but the BP86 functional has much larger AAD for the Rydberg excitations than for valence excitations, which is often cited as a problem of GGA functionals (see, however, the discussion below).

This special behavior of the GGAs for Rydberg excitations can be understood from the errors that are made by the LDA and GGA approximations in the orbital energy spectrum. It is known that the effect of the coupling matrix on the excitation energies is usually small[23] when "pure" DFT functionals are used (functionals that do not contain HF exchange), except in the cases of bond breaking and charge transfer excitations where the kernel term of the coupling matrix should be large (divergent),[33,34] but is not in the adiabatic approximation. So the orbital energy difference is a very good zero order approximation of the excitation energy for local molecular excitations. We will elaborate on this point in the next section. Here, we discuss the deficiency of the LDA/GGA approximations from their effect on the orbital energy spectrum, which is displayed in Figure 1.

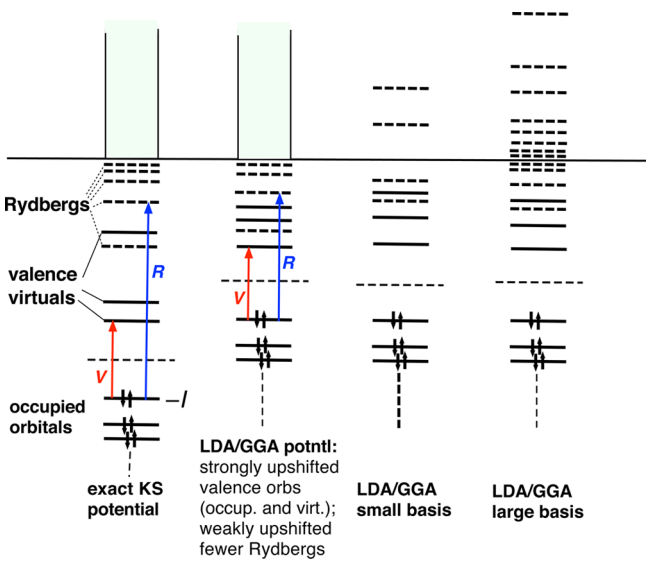

Figure 1. Schematic representation of the orbital energy spectrum of the exact Kohn−Sham potential, a typical GGA potential, and the approximate discrete LDA/GGA orbital energy spectra resulting from small and large basis set calculations. Drawn lines for valence orbitals, dashed lines for Rydberg levels. *V* denotes a valence excitation (HOMO to LUMO transition) and *R* denotes a Rydberg transition.

The orbital energy spectrum of the exact Kohn−Sham potential has the following characteristics: the HOMO is exactly at minus the first ionization potential, $\epsilon_H = -I$, the HOMO−LUMO gap is approximately equal to the first excitation energy or the optical gap (in molecules),[14] there is a series of Rydberg levels which converge to the energy zero from below,[35] and there is a continuous spectrum of free electron states above zero. The energy zero is always defined as the value of the KS potential at infinity, to give all potentials a common gauge and to be able to compare the orbital energy to the ionization energy, which is the energy required to bring an electron with zero kinetic energy to the asymptotic limit value of the potential. The nearly constant upshift of the GGA potentials of ca. 4.5 eV with respect to the exact potential in the molecular region leads to a similar, nearly uniform, upshift of the energies of the orbitals that have large amplitude in the molecular region, that is, the occupied orbitals and the unoccupied orbitals of valence type. Although this deficiency of the LDA/GGA potentials causes them to lose the property $\epsilon_i \approx -I_i$, which holds for the exact Kohn−Sham occupied orbital energies,[36−39] it does not affect the valence excitations very much, since also the valence virtuals shift up by approximately the same amount (note the near equality of the red valence excitation for the exact KS potential and LDA/GGA approximation in Figure 1). Therefore, GGAs work well for valence excitations, with similar AADs as more sophisticated potentials. The upshift of the somewhat more diffuse unoccupied valence orbitals may be slightly less than that of the occupied orbitals, giving the GGA calculations the tendency to slightly underestimate the valence excitations. The Rydberg orbitals, being mostly outside the molecular domain, shift up much less. Their orbital energies remain in the same energy region, since they will again by definition cluster toward the energy zero (from below) (but these potentials may support many fewer Rydberg-like orbitals). The Coulombic long-range decay of the exact potential $(-1/r)$ is not correctly reproduced by the LDA (exponential decay) and GGA $(-c/r^2)$ functionals.[40] This will deteriorate the shape of the Rydberg orbitals, which affects properties such as the oscillator strength.[29] However, more importantly, because of the smaller upshift of the Rydberg levels than the occupied orbitals, the orbital energy differences, which are the leading terms in the excitation energy by TDDFT, will become much too low, cf. the blue arrows for a Rydberg excitation in Figure 1. This causes GGA Rydberg excitation energies to be severely underestimated, see the large AADs for the BP86 Rydberg excitation energies in Table 1. These large underestimations of the Rydberg transitions have actually a second, even more serious, cause, see below. The problems with the GGA calculations have usually been ascribed to the wrong asymptotic behavior of the GGA potential and it has been proposed[22,23] to remedy the calculated excitation energies by using the asymptotically corrected potential LB94.[19] This potential had shown to considerably improve, for example, polarizabilities[20] and van der Waals interactions.[21] However, we wish to stress that the problem with GGA potentials is not in the wrong (non-Coulombic) decay of the potential in the asymptotic limit, it is actually in the wrong shape (erroneous upshift) of the GGA potential in the nearby (molecular) region. The important feature of the LB94 and SAOP potentials in the present context is their more strongly attractive nature in the molecular region (downshift with respect to the GGA potential) rather than their proper Coulombic asymptotic decay. [The SAOP potential is an improvement on the LB94 potential, which shares with LB94 the property that it does not have the erroneous upshift in the molecular region of the GGA potentials.] Tozer and Handy[24] have argued that the KS potential should asymptotically go to a positive (molecule dependent) constant and have applied a shape correction to the potential by leaving the GGA potential untouched in the molecular region, but connecting it to a long-range part that goes asymptotically to this positive constant. Even if one does not accept that there are physical arguments why the "right" GGA potential (or "continuum potential") should go to a molecule dependent constant at infinity, it can be recognized

dx.doi.org/10.1021/ct500727c | J. Chem. Theory Comput. XXXX, XXX, XXX−XXX

that the shape correction of ref 24 has the same effect: Since an overall constant in the potential is physically irrelevant, such a potential can be shifted uniformly down to put the asymptotic limit at zero. Such a downshift means that also the orbital levels shift down by this constant, which makes the orbital energies comparable to the orbital energies of the other shape-corrected potentials with asymptotic limit at zero.

The upshift of the GGA potential in the molecular region (with respect to the zero asymptotic limit) also leads to a strange basis set effect, that should not go unnoticed. In any basis, and in particular in a small basis set (see third column of Figure 1), the set of Rydberg levels is only very incompletely, and certainly for the upper Rydberg levels very poorly, represented. Moreover, the continuum above zero is only represented by a few discrete levels, which are artifacts of the basis set. When the basis set is increased, the Rydberg spectrum approaching zero from below and the continuous spectrum above zero are increasingly densely covered. In particular, the addition of diffuse functions will not only create more Rydberg-like solutions just below zero but also many one-electron states at positive energy close to zero, mimicking with these somewhat accidental discrete states the continuous spectrum of free-electron solutions. The correct free-electron solutions consist of plane waves orthogonalized to the bound orbitals. This means that upon enlarging the basis set the excitation spectrum becomes denser around the $I = -\epsilon_H$ value, with many of those excitations having a spurious nature. The "collapse" of the excitation spectrum above the $-\epsilon_H$ value was signaled by Casida et al.[22] Figure 2 provides an illustration where the eight excitation energies used in the benchmark calculations of refs 6 and 9 and the present ones are given for acetone for three functionals in a series of basis sets. Considering first BP86, it is clear that the first excitation, which is purely valence type ($n \rightarrow \pi^*$), is almost constant through the basis sets and is in good agreement with experiment (4.27 eV compared to 4.43 eV expt.). The second excitation energy stabilizes in the largest basis sets, although it is much too low compared to experiment (5.13 eV compared to 6.36 eV expt.). This is a Rydberg excitation ($n \rightarrow 3s$) to a diffuse orbital with energy (−0.61 eV) close to zero, but still bound. Its energy is too low because the HOMO is too high and therefore ($\epsilon_a - \epsilon_H$) too small. The remaining BP86 excitation energies clearly start clustering toward the $-\epsilon_H(BP86) \approx 5.7$ eV value from above, without much apparent connection to the experimental spectrum. One cannot obtain convergence of the GGA excitation spectrum with basis set, because the large upshift of the HOMO level brings the onset of the continuous part of the spectrum at a much too low energy, and the extension of the basis will only create more (spurious) orbitals and energies in the region above the energy zero. One should not assign these excitations as Rydberg excitations, since they are basically undefined orbitals. These orbitals are as diffuse as the basis set allows, the basis tries to mimic infinitely extended plane waves. Since the exchange-correlation kernel contribution for such (almost) infinitely extended orbitals is zero, the excitation energy tends to just the orbital energy difference $\epsilon_a - \epsilon_H \approx 0. - \epsilon_H$. These excitations have very small oscillator strengths; so in large basis sets with many diffuse functions, one should be alerted by many spurious excitations with very small oscillator strengths. In small basis sets, there are fewer discrete levels above zero, but the corresponding excitations are still spurious (artifacts of the basis). It is to be noted that when doing benchmarking of functionals it should be recognized which excitation energies are "stable" and can be included in the benchmarking and which ones are spurious. The result of benchmarking of LDA/GGA/mGGA functionals is unrealistic if these problems with

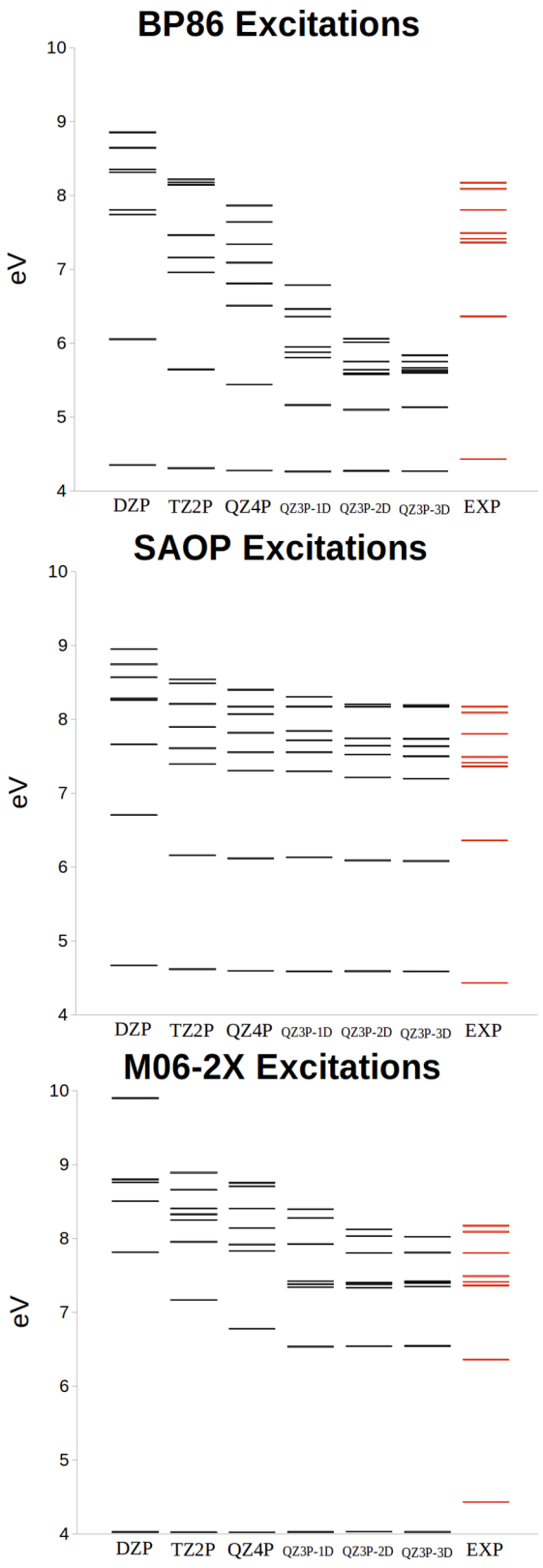

Figure 2. Lowest 8 excitation energies of acetone used in the benchmark calculations of refs 6 and 9 as a function of basis set size, for BP86 functional (a), SAOP functional (b), and M06-2X functional (c).

dx.doi.org/10.1021/ct500727c | J. Chem. Theory Comput. XXXX, XXX, XXX−XXX

Table 2. Results for the Excitations Used in the Benchmark Articles for the Acetone Molecule (Basis: QZ3P-2D)[a]

state	type	W	ϵ_i	ϵ_a	$\Delta\epsilon_{ia}$	E_{exp}	ω	$\omega - \Delta\epsilon_{ia}$	$\omega - E_{exp}$
				SAOP					
1^1A_2	V	1.00	−10.25	−5.92	4.33	4.43	4.59	0.26	0.16
1^1B_2	R	1.00	−10.25	−4.18	6.07	6.36	6.09	0.02	−0.27
2^1A_2	R	0.84	−10.25	−2.72	7.53	7.36	7.52	0.00	0.16
2^1A_1	R	0.97	−10.25	−3.09	7.16	7.41	7.21	0.05	−0.20
2^1B_2	R	0.97	−10.25	−2.63	7.62	7.49	7.64	0.02	0.15
3^1A_1	R	0.97	−10.25	−2.04	8.21	7.80	8.20	0.00	0.40
3^1B_2	R	0.97	−10.25	−2.51	7.74	8.09	7.74	0.00	−0.35
2^1B_1	R	0.97	−10.25	−1.83	8.42	8.17	8.43	0.01	0.26
				BP86					
1^1A_2	V	1.00	−5.71	−1.70	4.01	4.43	4.27	0.26	−0.16
1^1B_2	R	1.00	−5.71	−0.61	5.10	6.36	5.10	0.00	−1.26
2^1A_2	R	1.00	−5.71	−0.11	5.60	7.36	5.59	0.00	−1.77
2^1A_1	R	1.00	−5.71	−0.13	5.58	7.41	5.58	0.00	−1.83
2^1B_2	R	1.00	−5.71	−0.07	5.64	7.49	5.64	−0.01	−1.85
3^1A_1	R	0.98	−5.71	0.36	6.07	7.8	6.06	−0.01	−1.74
3^1B_2	R	1.00	−5.71	0.05	5.76	8.09	5.75	0.00	−2.34
1^1B_1	R	1.00	−5.71	0.31	6.02	8.17	6.01	−0.01	−2.16
				TDHF					
1^1A_2	V	0.47	−11.23	3.96	15.18	4.43	5.03	−10.15	0.60
1^1B_2	R	0.36	−11.23	0.62	11.85	6.36	8.24	−3.61	1.88
2^1A_2	R	0.43	−11.23	1.02	12.25	7.36	9.02	−3.23	1.66
2^1A_1	R	0.20	−11.23	0.96	12.19	7.41	9.07	−3.12	1.66
2^1B_2	R	0.31	−11.23	1.20	12.43	7.49	9.13	−3.30	1.64
3^1A_1	R	0.21	−13.20	3.96	17.15	7.8	9.41	−7.74	1.61
3^1B_2	R	0.23	−11.23	1.74	12.96	8.09	9.59	−3.37	1.50
1^1B_1	R	0.29	−15.23	3.96	19.18	8.17	9.66	−9.52	1.49
				M06-2X					
1^1A_2	V	0.52	−8.85	0.78	9.63	4.43	4.03	−5.60	−0.40
1^1B_2	R	0.73	−8.85	−0.34	8.51	6.36	6.54	−1.97	0.18
2^1A_2	R	0.62	−8.85	0.04	8.88	7.36	7.33	−1.55	−0.03
2^1A_1	R	0.62	−8.85	0.03	8.87	7.41	7.38	−1.49	−0.03
2^1B_2	R	0.45	−8.85	0.15	9.00	7.49	7.40	−1.60	−0.09
3^1A_1	R	0.79	−8.85	0.74	9.58	7.80	8.03	−1.55	0.23
3^1B_2	R	0.42	−8.85	0.64	9.49	8.09	7.80	−1.69	−0.29
1^1B_1	R	0.92	−8.85	0.73	9.58	8.17	8.12	−1.45	−0.05

[a]W(eight) = contribution of the largest single orbital to orbital transition to the total excitation vector, ϵ_i = donor orbital energy (usually the HOMO), ϵ_a = acceptor orbital energy, $\Delta\epsilon_{ia}$ = orbital energy difference, ω = calculated excitation energy, E_{exp} = experimental excitation energy. V stands for valence, R for Rydberg character. The 1^1A_2 state is considered to have valence-like character, while other states are considered to be Rydberg states. Experimental (adiabatic) ionization energy: 9.71 eV.[41,42]

excitations to the continuum part of the spectrum (above the much too low $-\epsilon_{HOMO}$ value) are not recognized and the spurious excitations are included in the benchmark set.

We note in the acetone results that the SAOP potential does not suffer from this peculiar deficiency. Since the HOMO is at −10.25 eV, the eight excitations we are considering are all to negative energy (bound) orbitals (see the ϵ_a values in Table 2), which should have stable shapes and energies in sufficiently large basis sets. This is evident from Figure 2b. Although the DZP basis is clearly too small, the calculated excitation energies are reasonably stable from the TZ2P basis onward for all excited states. This does not necessarily mean that the calculated energies are excellent, but they are quite reasonable and stable. It is interesting to compare to the results for hybrid functionals, for which we take M06-2X as representative, see Figure 2c. Clearly, the M06-2X levels are more stable than BP86. The HOMO is at −8.85 eV, which represents an upshift of only ca. 0.9 eV with respect to the (adiabatic) ionization potential of 9.71 eV.[41,42] We expect therefore somewhat too low excitation energies for high lying Rydberg transitions, which indeed seems to be a tendency with the M06-2X highest excitation energies. Most of the excitations (except the lowest two) are to orbitals with positive energy (Table 2), but the calculated excitation energies are well below the 8.85 eV threshold. Because of the exact exchange contribution in this functional, the exchange-correlation kernel has much larger contributions (cf. the large $\omega - \Delta\epsilon_{ia}$ values in Table 2) than in the case of purely local functionals such as BP86 and SAOP. This apparently corrects for the spurious nature of the positive energy orbitals and results in good excitation energies.

We emphasize that not only the numerical values for the excitation energies are important. Also the nature of the excitations, as given by the percentage contributions of the $i \rightarrow a$ (occupied to virtual) excitations to the transition density, is an important characteristic that should not be distorted by approximations in the functional/potential. This is discussed in the next section.

dx.doi.org/10.1021/ct500727c | J. Chem. Theory Comput. XXXX, XXX, XXX−XXX

III. SINGLE EXCITATION NATURE (ORBITAL-TO-ORBITAL TRANSITION) OF MANY EXCITATIONS IN THE KOHN−SHAM BASIS

The problems highlighted in the previous section do not arise with the exact Kohn−Sham potential. Since this is not available, a model potential that approximates a crucial feature of the exact KS potential such as the $\epsilon_H = -I$ relation should be used. The statistical average of model potentials (SAOP)[15−17,29] is such a purely local potential, with a reasonable approximation of $\epsilon_H = -I$.[36]

In case of exact KS DFT, the orbital energy difference $\epsilon_a - \epsilon_i$ is expected to be a good approximation to the actual excitation energy for local molecular excitations, because of the physical meaning of the KS orbital energies.[14] The occupied orbitals ϵ_i are approximately equal to ionization potentials (IP) for the valence orbitals,[36,43−45] with deviations for the upper valence orbitals of the order of magnitude of 0.1 eV (the HF model gives deviations of the orbital energies from ionization energies for those levels of ca. 1 eV). The approximation $\epsilon_i \approx -I_i$ becomes an exact equality for the HOMO orbital energy and first IP.[40,46] The virtual orbital energies ϵ_a belong to higher states of an electron in exactly the same KS potential as the occupied orbitals, so they represent excited KS electrons. This is truly different from the meaning of unoccupied orbitals in the Hartree−Fock model, which describe electrons that are added to the system. The unoccupied HF orbital energies are Koopmans (frozen orbital) approximations to the electron affinity (actually poorer than the Koopmans approximation of the occupied HF orbital energies to the IPs, because for the virtuals the relaxation and correlation errors add up while for the occupied orbitals they counteract, cf.[14]). The difference between KS and HF virtual orbitals and orbital energies can be understood as the effect of the exchange-correlation hole potential, which is present in the v_{xc} part of the KS potential and causes the KS electrons to move in the field of $N - 1$ electrons, both in occupied and in virtual orbitals. In contrast, the Fock operator for the virtual orbitals does not have an exchange hole potential, the virtual HF orbitals describe an electron moving in the field of N electrons, which makes the orbitals much more diffuse. The difference of the virtual-occupied KS orbital energies should give a good zero order estimate of the energy required to excite an electron from an occupied orbital to a virtual orbital, to the extent that the KS system of electrons mimics the true system. [The orbital energy difference estimate breaks down in the case of charge transfer excitations[14,33,47] and bond breaking excitations[34,48] and, in general, when the KS independent particle system deviates strongly from the true system with strong nondynamic correlation (multideterminantal character).] For local functionals (GGA etc.), the orbital energy difference may still be a good estimate for low lying excitations, but this estimate is expected to break down for higher excitations that exceed or approach the $-\epsilon_H$ threshold, see ref 22 and the discussion in the previous section.

We give in Table 2 for various functionals the same eight excitations of acetone as used in refs 6 and 9, which are to one valence and seven Rydberg states. Assignment of valence states is usually easy from the orbitals involved in the transition, but Rydberg states are more difficult to assign. For them, we stick to the convention of simply matching, per irreducible representation, the calculated to the experimental excitations in order of energy, see remarks in refs 6 and 9. Of course, the characterization as valence (V) or Rydberg (R) is not absolute; there are many mixed cases. In the case of acetone, only the lowest of the present states, 1^1A_2 ($n \rightarrow \pi^*$), is considered valence.[6,9] We use acetone here as just an example, and we will refrain from a discussion of assignment issues in any depth, except for a few remarks, see below.

In the first place, we note that the expectation that the KS orbital energy differences $\Delta\epsilon_{ia}$ (for which we take the SAOP model) are close to the calculated TDDFT excitation energies is fully borne out: the discrepancies listed as $\omega - \Delta\epsilon_{ia}$ are extremely small. This is equivalent to saying that the contributions of the exchange-correlation kernel are very small (a few hundredths of an eV). Of course we cannot be sure that these contributions, for which we take the adiabatic LDA approximation, are quantitatively correct, but for Rydberg excitations, there is only a small differential overlap of ϕ_i and ϕ_a^{Rydberg}, so the factor $\phi_i(\boldsymbol{r})\phi_a^{\text{Rydberg}}(\boldsymbol{r})$ in the integrand of the exchange-correlation kernel is ≈0 everywhere and the kernel contribution will be small anyway. For the lowest excitation, 1^1A_2, which is HOMO → LUMO, there is some contribution (0.26 eV) from the exchange-correlation kernel. This is in keeping with the valence character of the excitation, so the differential overlap $\phi_i(\boldsymbol{r})\phi_a^{\text{val}}(\boldsymbol{r})$ will not be so small as for Rydberg excitations. Nevertheless, the kernel term is still so small as to make the orbital energy difference a quite good approximation to the calculated excitation energy. It is, in fact, an important advantage of the use of a good approximation to the exact KS potential that orbital energy differences are meaningful and in fact very good first approximations to the excitation energies. Another important advantage of the KS potential (or a good approximation to it) is also apparent from the SAOP results of Table 2: the character of all of the excitations is completely unequivocally just a single orbital transition. The weights for the dominant single excitation are 95% or higher for all excitations except 2^1A_2 (84%). All of the excitations are out of the HOMO (the $2p_y$ lone pair on oxygen). The physical nature of all of the excitations is apparently very straightforward in the KS orbital basis. This underlines our earlier remark that from the nature of the KS potential the virtual KS orbitals can be expected to approximately describe excited electrons in the system. This simple and straightforward description of excitations is a great advantage of the KS (SAOP) orbital basis. We finally note that the agreement of the calculated excitation energies with experiment is very satisfactory.

We note in passing that the assignment of the acetone spectrum is not at all simple.[41,42,49−52] The excitations we are considering here are generally considered to be, except for the lowest (the $n \rightarrow \pi^*$ valence excitation), Rydberg excitations to 3s, 3p_x, 3p_y, 3p_z and next to the 3d set. However, also, the valence $\pi \rightarrow \pi^*$ and $\sigma \rightarrow \pi^*$ excitations should occur. They have been experimentally rather elusive. From theoretical work[49] it became clear that, as expected, such states have considerably lengthened equilibrium C═O bonds and potential energy curves that exhibit avoided crossings with sometimes several Rydberg states. Experimentally, the existence of the valence $\pi \rightarrow \pi^*$ and $\sigma \rightarrow \pi^*$ states has been deduced from the vibronic coupling,[49−51] but vertical excitation energies have been difficult to ascertain. We have followed refs 6 and 9 in considering the one valence and seven Rydberg states mentioned above.

Turning to the GGA functional BP86, we note that in spite of the too high lying HOMO (at −5.71 eV compared to the IP

dx.doi.org/10.1021/ct500727c | J. Chem. Theory Comput. XXXX, XXX, XXX−XXX

Table 3. Results for the Six Excitations Used in the Benchmark Articles for the Pyrimidine Molecule (Basis: QZ3P-2D), Which Are All Excitations to the π^* Manifold[a]

state	type	W	ϵ_i	ϵ_a	$\Delta\epsilon_{ia}$	ω	$\omega - \Delta\epsilon_{ia}$	$\omega - E_{exp}$
				SAOP				
1^1B_1	V	1.00	−10.30	−6.52	3.78	3.97	0.19	0.12
1^1A_2	V	0.98	−10.30	−6.12	4.19	4.27	0.09	−0.35
1^1B_2	V	0.74	−11.45	−6.52	4.93	5.57	0.64	0.45
2^1A_2	V	0.98	−11.54	−6.52	5.02	5.27	0.24	−0.25
2^1B_1	V	0.99	−11.54	−6.12	5.43	5.57	0.15	−0.33
1^1A_1	V	0.76	−11.45	−6.12	5.33	6.44	1.12	−0.26
				BP86				
1^1B_1	V	0.99	−6.03	−2.42	3.61	3.80	0.19	−0.05
1^1A_2	V	0.99	−6.03	−2.07	3.96	4.04	0.08	−0.58
1^1B_2	V	0.72	−7.41	−2.42	4.98	5.58	0.60	0.46
2^1A_2	V	0.98	−7.28	−2.42	4.86	5.11	0.26	−0.41
2^1B_1	V	0.99	−7.28	−2.07	5.21	5.35	0.15	−0.55
1^1A_1	V	0.71	−7.41	−2.07	5.33	6.44	1.11	−0.26
				M06-2X				
1^1B_1	V	0.95	−8.92	−0.49	8.42	4.26	−4.17	0.41
1^1A_2	V	0.93	−8.92	−0.15	8.77	4.75	−4.01	0.13
1^1B_2	V	0.77	−9.43	−0.49	8.94	5.72	−3.22	0.60
2^1A_2	V	0.91	−10.31	−0.49	9.82	5.73	−4.09	0.21
2^1B_1	V	0.94	−10.31	−0.15	10.16	6.21	−3.96	0.31
1^1A_1	V	0.69	−9.43	−0.15	9.28	6.37	−2.91	−0.33
				TDHF				
1^1B_1	V	0.73	−11.31	2.20	13.51	5.70	−7.81	1.85
1^1A_2	V	0.29	−11.31	2.61	13.92	6.38	−7.54	1.76
1^1B_2	V	0.69	−10.21	2.20	12.41	6.12	−6.29	1.00
2^1A_2	V	0.63	−12.87	2.20	15.07	7.30	−7.77	1.78
2^1B_1	V	0.49	−10.21	0.68	10.89	7.32	−3.57	1.42
1^1A_1	V	0.52	−10.21	0.63	10.84	8.19	−2.65	1.49

[a]W(eight) = contribution to the total excitation vector of the largest orbital to orbital transition, ϵ_i = donor orbital energy, ϵ_a = acceptor orbital energy, $\Delta\epsilon_{ia}$ = orbital energy difference, ω = calculated excitation energy, E_{exp} = experimental excitation energy. All excitations have valence (V) character. Experimental ionization energy: 9.23 eV[58].

of 9.71 eV[41,42]), the valence excitation 1^1A_2 is not much affected: the LUMO has been upshifted by about the same amount as the HOMO, so $\Delta\epsilon_{ia}$ is still close to the excitation energy (actually 0.16 eV smaller, while with SAOP it was 0.16 eV larger, cf. the tendency of smaller upshift of the valence virtuals we mentioned earlier). All of the other excitations are to orbitals that are either a little below or above zero (Table 2). The ones above zero are spurious, since the positive orbital energies are artifacts of the basis. The ones at negative orbital energy are close to zero (from −0.61 to −0.07 eV). It is not clear whether these are good approximations to Rydberg orbitals, given the limited extent of the basis functions and the wrong asymptotic decay of the potential. They are very diffuse, which yields a zero contribution from the kernel term and therefore also 100% single orbital excitation character. The calculated excitation energies are all much too low (see the column $\omega - E_{exp}$), since they cluster around the $-\epsilon_H$ value as discussed in the previous section. It is doubtful if these excitations are at all realistic, and whether they can be used for judging (benchmarking) this GGA functional.

We next consider the TDHF (RPA) excitations. Here, we find *all* virtual levels at positive orbital energies. Those orbitals are again arbitrary products of the basis set, devoid of physical meaning. Indeed, the excitation vectors are extensive mixtures of the $\phi_i \rightarrow \phi_a$ orbital transitions, with the largest contribution sometimes as low as 20%. Meaningful interpretation of the nature of these excitations appears well-nigh impossible, while judging from the Kohn−Sham (SAOP) calculations their character is actually very simple. The 1^1A_2 excitation, which is denoted "valence", actually has in TDHF less than 50% contribution from the HOMO to LUMO + 27 ($n \rightarrow \pi^*$) character. The lowest B_1 state has 29% HOMO − 4 (σ) to LUMO + 27 character, so has some $\sigma \rightarrow \pi^*$ character and is not totally Rydberg. Although interpretation is obviously difficult for the TDHF calculations because of the unphysical nature of the orbitals with positive energy, numerically, the excitation energies can be meaningful. After all, the excited states are bound states and can be described with molecule centered basis sets. Of course, large corrections then have to come from the exchange kernel contributions. These contributions are indeed large, cf. the large differences $\omega - \epsilon_{ia}$ in Table 2. Nevertheless, the errors of the calculated excitation energies are all large; in this case, the deviations are positive (to too high energies) by about as much as the BP86 deviations were negative.

Given the trouble with the GGAs and the pure-exchange TDHF method in these response calculations, it is interesting to see what a hybrid method does. An averaging of the GGA and TDHF results, as may be expected from a hybrid method, would already lead to improvement. We present in the tables the results for the M06-2X method, which was the best functional in ref 9. Indeed, we observe that the calculated excitation energies are excellent, the best of the functionals that are compared here. On the other hand, this functional, just as

dx.doi.org/10.1021/ct500727c | J. Chem. Theory Comput. XXXX, XXX, XXX−XXX

the GGA and HF models, suffers from many orbital energies being positive. In fact, only the LUMO is at negative orbital energy ($9a_1$ at −0.34 eV). The character of the virtual orbitals may therefore be dubious. The excitations are no longer of almost pure single-excitation character, as they were with SAOP and BP86. The composition of the excitations is, as expected, in between the GGA and TDHF cases: many of the transitions are strongly mixed, but the mixing is less extensive than in the TDHF case. The exchange correlation kernel contribution is smaller than in the case of TDHF but still large. The orbital energy differences are therefore not good indicators of the excitation energies, cf. the first excited state (the valence 1^1A_2) with $\Delta\epsilon_{ia}$ = 9.63 and a correction of −5.60 to obtain the calculated excitation energy of 4.03 eV.

We note that the problems we have been discussing with GGA calculations are not severe for the low lying excitations if they are well below the $-\epsilon_{\mathrm{HOMO}}$ threshold. As an example we give in Table 3 results for the pyrimidine molecule, for the lowest six excitations (following refs 6, 9, and 53), which are all of valence type. We use the benchmark values used in refs 6 and 9. [It should be noted that there are differences of 0.3−0.7 eV with Thiel et al.'s best estimates,[53] which may serve as a *caveat* against overinterpretation of the comparison of the TDDFT results with these benchmark values.] We again observe good results for the SAOP calculations. The errors with experiment are slightly larger on average than for acetone. The differences of the calculated excitation energies with the orbital energy gaps $\Delta\epsilon_{ia}$ are now a bit larger. This is because acetone has mostly Rydberg states, for which the kernel contribution is very small so the orbital energy differences are extremely good zero-order estimates of the calculated excitation energies. The present excitations of pyrimidine are all valence type, so the very small $(\omega - \Delta\epsilon_{ia})$ values that are typical for Rydberg transitions are now absent, but still, the $(\omega - \Delta\epsilon_{ia})$ differences are small and the orbital energy differences are reasonably close to the excitation energies. The excitations are also predominantly single orbital transition type. This is pleasing from the point of view of interpretation, but we stress that it is definitely possible that valence excited states consist of more than one single excitation: it sometimes happens that an excited state is physically a strong mixture of a few orbital excitations. This is, for instance, the case for the lowest excitations of porphyrines and phthalocyanines (Q-band and B band), which are basically transitions within the set of four Gouterman orbitals.[54] These have been early examples where it was demonstrated that TDDFT can perfectly handle such situations.[55,56] We note that for BP86 the current six pyrimidine excitations are all below the $-\epsilon^{\mathrm{BP86}}_{\mathrm{HOMO}}$ threshold and do not have any problem: they are all to virtual orbitals with negative orbital energy, the excitation energies are fairly close to orbital energy differences, and they are all predominantly composed of a single orbital excitation. The TDHF transitions on the other hand are all to virtual orbitals with positive orbital energy and show considerable mixing of single excitations. The orbital energy differences are far off the excitation energies. The M06-2X calculations are to orbitals with negative (although rather small) orbital energies; they still have, as do SAOP and BP86, predominantly single orbital excitation character, but the orbital energy differences are again far from the excitation energies and the $(\omega - \Delta\epsilon_{ia})$ correction terms from the kernel are large. TDHF excitation energies are numerically not accurate. The M06-2X ones are much better, of similar accuracy as SAOP and BP86. This example underlines that for excitations well below the $-\epsilon_{HOMO}$ threshold all TDDFT methods perform similarly as far as excitation energies are concerned. If (benchmark-) studies are restricted to only low-lying excitations,[1,3,4,7,11−13] which are often the relevant excitations in important chromophores, the application of the standard approximate Kohn−Sham potentials will not do much harm as far as the calculated excitation energies and the composition of the excited states are concerned.

IV. CONCLUDING REMARKS

We have advocated in this paper the use of an accurate approximation to the exact Kohn−Sham potential for use in TDDFT calculations for excitations, such as the SAOP potential,[15,16,29] for the following reasons. (1) The KS orbital energies approximate the excitation energies often quite closely as virtual minus occupied orbital energy differences. (2) The character of the excitations is very often just a single orbital transition (or very few orbital transitions) in the KS orbital basis, in accordance with the physical meaning of the exact virtual KS orbitals. (3) The bound excited states below the ionization threshold are amenable to TDDFT treatment because the relevant virtual orbitals are bound one-electron states in the KS potential. We have contrasted these properties with those of approximate functionals, both hybrid and GGA. In particular, the latter suffer from a wrong much too low $-\epsilon_{\mathrm{HOMO}}$ and accordingly many spurious excitations at higher energies than $-\epsilon_{\mathrm{HOMO}}$ (cf. ref 22). The hybrid functionals suffer from the interpretation problem (which is very extreme with the 100% exchange TDHF method) arising from the mixing of orbital excitations caused by the unphysical nature of the positive energy virtual orbitals.

It is often stated that "TDDFT has a problem with Rydberg transitions". This statement should be qualified: there is nothing problematic with the calculation of Rydberg excitation energies, provided a good enough approximation to the Kohn−Sham potential is used to calculate the bound Rydberg orbitals and their orbital energies. Rydberg excited states are even especially simple, the exchange-correlation kernel term making only a very small contribution, because the differential overlap of the tight valence and diffuse Rydberg orbitals is small: $\phi_i(\boldsymbol{r})\phi_a(\boldsymbol{r}) \approx 0$. "A good enough approximation" means that in particular the property of the KS potential that it incorporates the potential of the (coupling constant integrated) exchange-correlation hole comprising −1 electron, which gives it a $-1/r$ tail, is properly included. Evidently, that property is crucial for the very diffuse Rydberg orbitals. With the exact Kohn−Sham potential, which is, for example, available for He and Be, the orbital energies give such a good approximation for Rydberg transition energies that even the quantum defect can be determined![35]

A clear distinction should be made between the problems of charge-transfer and those of Rydberg excitations. Rydberg excitations are purely a problem of a poor approximation to the KS potential. With the exact or with an accurate KS potential, the one-electron energies should be accurate, and since the kernel contribution becomes very small, the adiabatic TDDFT method is very accurate. This is exemplified by the present SAOP results, earlier very accurate KS potential results for a few molecules[23] and earlier exact KS potential results for He and Be.[35] Charge transfer excitations are on the other hand fundamentally a problem of the exchange-correlation kernel; these excitations are not well approximated by even the exact KS orbital energy difference and TDDFT in this case needs

large corrections to the adiabatic LDA/GGA exchange-correlation kernel in order to calculate correctly the large difference between the orbital energy difference and the accurate transition energies.[14,33] The charge transfer problem is not a problem of the GGA approximation of the KS potential (e.g., its lack of derivative discontinuity jump), but it is a deficiency of the GGA approximation to the exchange-correlation kernel.

The problem that GGAs have with Rydberg transitions has nothing to do with the nature of the orbitals involved, it is simply caused by the wrong (too high) orbital energy of the HOMO. The bound Rydberg states in the GGA potential, close to zero, will have too low excitation energies because of the too small $\Delta\epsilon_{ia}$ gap. All transitions above the $-\epsilon_{\mathrm{HOMO}}$ threshold, also those of valence type, are compromised.

The fact that the KS HOMO−LUMO gap in molecules, which is reproduced rather well with LDA and GGA potentials, differs very much from the one in Hartree−Fock, that is, is not an approximation to ionization energy (I) minus electron affinity (A), is often referred to as "the band gap problem" of DFT. However, the HOMO−LUMO gap of the KS model is physically an approximation to the lowest excitation energy, which is a beautiful property. There is nothing problematic about it. The situation in solids is more subtle.[14,57]

■ ASSOCIATED CONTENT

Supporting Information

Tables with the calculated excitation energies for the 11 molecules for which the same excitations have been calculated as in refs 6 and 9. This material is available free of charge via the Internet at http://pubs.acs.org/.

■ AUTHOR INFORMATION

Corresponding Author

*Email: e.j.baerends@vu.nl.

Notes

The authors declare no competing financial interest.

■ ACKNOWLEDGMENTS

This work was supported by Chemical Sciences of The Netherlands Organization for Scientific Research (NWO−CW, grant No. ECHO 712.011.001) (R.v.M.), and by the WCU (World Class University) program (E.J.B., O.V.G.) through the Korea Science and Engineering Foundation funded by the Ministry of Education, Science and Technology of the Republic of Korea (Project No. R32-2008-000-10180-0). We gratefully acknowledge the computer time provided by the NWO Foundation for National Computing Facilities at SARA, Amsterdam.

■ REFERENCES

(1) Silva-Junior, M. R.; Schreiber, M.; Sauer, S. R.; Thiel, W. *J. Chem. Phys.* **2008**, *129*, 104103.
(2) Rohrdanz, M. A.; Herbert, J. M. *J. Chem. Phys.* **2008**, *129*, 034107.
(3) Jacquemin, D.; Wathelet, V.; Perpète, E. A.; Adamo, C. *J. Chem. Theor. Comp.* **2009**, *5*, 2420−2435.
(4) Goerigk, L.; Grimme, S. *J. Chem. Phys.* **2010**, *132*, 184103.
(5) Jacquemin, D.; Perpète, E. A.; Ciofini, I.; Adamo, C.; Valero, R.; Zhao, Y.; Truhlar, D. G. *J. Chem. Theor. Comp.* **2010**, *6*, 2071−2085.
(6) Caricato, M.; Trucks, G. W.; Frisch, M. J.; Wiberg, K. B. *J. Chem. Theor. Comp.* **2010**, *6*, 370−383.
(7) Send, R.; Kühn, M.; Furche, F. *J. Chem. Theor. Comp.* **2011**, *7*, 2376−2386.
(8) Peverati, R.; Truhlar, D. G. *J. Phys. Chem. Lett.* **2011**, *2*, 2810−2817.
(9) Isegawa, M.; Peverati, R.; Truhlar, D. G. *J. Chem. Phys.* **2012**, *137*, −.
(10) Leang, S. S.; Zahariev, F.; Gordon, M. S. *J. Chem. Phys.* **2012**, *136*, 104101.
(11) Jacquemin, D.; Planchat, A.; Adamo, C.; Menucci, B. *J. Chem. Theor. Comp.* **2012**, *8*, 2359−2372.
(12) Adamo, C.; Jacquemin, D. *Chem. Soc. Rev.* **2013**, *42*, 845−856.
(13) Fang, C.; Oruganti, B.; Durbeej, B. *J. Phys. Chem. A* **2014**, *118*, 4157−4171.
(14) Baerends, E. J.; Gritsenko, O. V.; van Meer, R. *Phys. Chem. Chem. Phys.* **2013**, *15*, 16408−16425.
(15) Gritsenko, O. V.; Schipper, P. R. T.; Baerends, E. J. *Chem. Phys. Lett.* **1999**, *302*, 199−207.
(16) Schipper, P. R. T.; Gritsenko, O. V.; van Gisbergen, S. J. A.; Baerends, E. J. *J. Chem. Phys.* **2000**, *112*, 1344.
(17) Grüning, M.; Gritsenko, O. V.; van Gisbergen, S. J. A.; Baerends, E. J. *J. Chem. Phys.* **2001**, *114*, 652−660.
(18) Casida, M. E. In *Recent Advances in Density-Functional Methods, Part I*; Chong, D. P., Ed.; World Scientific: Singapore, 1995; p 155.
(19) van Leeuwen, R.; Baerends, E. J. *Phys. Rev. A* **1994**, *49*, 2421.
(20) van Gisbergen, S. J. A.; Osinga, V. P.; Gritsenko, O. V.; van Leeuwen, R.; Snijders, J. G.; Baerends, E. J. *J. Chem. Phys.* **1995**, *105*, 3142−3151.
(21) Osinga, V. P.; van Gisbergen, S. J. A.; Snijders, J. G.; Baerends, E. J. *J. Chem. Phys.* **1997**, *106*, 5091.
(22) Casida, M. E.; Jamorski, C.; Casida, K. C.; Salahub, D. R. *J. Chem. Phys.* **1998**, *108*, 4439−4449.
(23) van Gisbergen, S. J. A.; Kootstra, F.; Schipper, P. R. T.; Snijders, J. G.; Gritsenko, O. V.; Baerends, E. J. *Phys. Rev. A* **1998**, *57*, 2556.
(24) Tozer, D.; Handy, N. C. *J. Chem. Phys.* **1998**, *109*, 10180−10189.
(25) van Gisbergen, S. J. A.; Snijders, J. G.; Baerends, E. J. *J. Chem. Phys.* **1998**, *109*, 10657−10668.
(26) Hesselmann, A.; Jansen, G. *Chem. Phys. Lett.* **2002**, *362*, 319.
(27) Misquitta, A. J.; Jeziorski, B.; Szalewicz, K. *Phys. Rev. Lett.* **2003**, *91*, 1−4.
(28) Almbladh, C.-O.; Pedroza, A. C. *Phys. Rev. A* **1984**, *29*, 2322.
(29) Grüning, M.; Gritsenko, O.; van Gisbergen, S. J. A.; Baerends, E. J. *J. Chem. Phys.* **2002**, *116*, 9591−9601.
(30) Gritsenko, O. V.; van Leeuwen, R.; van Lenthe, E.; Baerends, E. J. *Phys. Rev. A* **1995**, *51*, 1944−1954.
(31) Petersilka, M.; Gossmann, U. J.; Gross, E. K. U. *Phys. Rev. Lett.* **1996**, 1212−1215.
(32) Ullrich, C. A.; Gossmann, U. J.; Gross, E. K. U. *Phys. Rev. Lett.* **1995**, *74*, 872−875.
(33) Gritsenko, O.; Baerends, E. J. *J. Chem. Phys.* **2004**, *121*, 655.
(34) Giesbertz, K. J. H.; Baerends, E. J. *Chem. Phys. Lett.* **2008**, *461*, 338.
(35) Savin, A.; Umrigar, C. J.; Gonze, X. *Chem. Phys. Lett.* **1998**, *228*, 391−395.
(36) Chong, D. P.; Gritsenko, O. V.; Baerends, E. J. *J. Chem. Phys.* **2002**, *116*, 1760.
(37) Gritsenko, O. V.; Baerends, E. J. *J. Chem. Phys.* **2002**, *117*, 9154.
(38) Gritsenko, O. V.; Braïda, B.; Baerends, E. J. *J. Chem. Phys.* **2003**, *119*, 1937.
(39) Gritsenko, O. V.; Baerends, E. J. *J. Chem. Phys.* **2004**, *120*, 8364−72.
(40) Almbladh, C.-O.; von Barth, U. *Phys. Rev. B* **1985**, *31*, 3231−3244.
(41) Furuya, K.; Katsumata, S.; Kimura, K. *J. Electron Spectr. Relat. Phen.* **1993**, *62*, 237−243.
(42) Wiedmann, R. T.; Goodman, L.; White, M. G. *Chem. Phys. Lett.* **1998**, *293*, 391−396.
(43) Gritsenko, O. V.; Baerends, E. J. *J. Chem. Phys.* **2002**, *117*, 9154−9159.
(44) Gritsenko, O. V.; Braïda, B.; Baerends, E. J. *J. Chem. Phys.* **2003**, *119*, 1937.

(45) Gritsenko, O. V.; Baerends, E. J. *J. Chem. Phys.* **2004**, *120*, 8364−72.
(46) Levy, M.; Perdew, J. P.; Sahni, V. *Phys. Rev. A* **1984**, *30*, 2745.
(47) Dreuw, A.; Weisman, J. L.; Head-Gordon, M. *J. Chem. Phys.* **2003**, *119*, 2943.
(48) Gritsenko, O.; van Gisbergen, S. J. A.; Görling, A.; Baerends, E. J. *J. Chem. Phys.* **2000**, *113*, 8478.
(49) Merchán, M.; Roos, B. O.; McDiarmid, R.; Xing, X. *J. Chem. Phys.* **1996**, *104*, 1791−1804.
(50) ter Steege, D. H. A.; Wirtz, A. C.; Buma, W. J. *J. Chem. Phys.* **2002**, *116*, 547−560.
(51) Nobre, M.; Fernandes, A.; Ferreira da Silva, F.; Antunes, R.; Almeida, D.; Kokhan, V.; Hoffmann, S. V.; Mason, N. J.; Eden, S.; Limao-Vieira, P. *Phys. Chem. Chem. Phys.* **2008**, *10*, 550−560.
(52) Lavín, C.; Velasco, A. M. *J. Quant. Spectr. Rad. Transfer* **2013**, *127*, 96−101.
(53) Schreiber, M. R.; Silva-Junior, M.; Sauer, S. P. A.; Thiel, W. *J. Chem. Phys.* **2008**, *128*, 134110.
(54) Sayer, P.; Gouterman, M.; Connell, C. R. *Acc. Chem. Res.* **1982**, *15*, 73.
(55) van Gisbergen, S. J. A.; Rosa, A.; Ricciardi, G.; Baerends, E. J. *J. Chem. Phys.* **1999**, *111*, 2499−2506.
(56) Rosa, A.; Ricciardi, G.; Baerends, E. J.; van Gisbergen, S. J. A. *J. Phys. Chem. A* **2001**, *105*, 3311−3327.
(57) Kuisma, M.; Ojanen, J.; Enkovaara, J.; Rantala, T. T. *Phys. Rev. B* **2010**, *82*, 115106.
(58) Lide, D. P., Ed. *CRC Handbook of Chemistry and Physics*, 90th ed.; CRC Press/Taylor and Francis: Boca Raton, FL, 2010; p 10.215.